Adsorptive remediation of naproxen from water using in-house developed hybrid material functionalized with iron oxide

Juliana Heloisa Pinê Américo-Pinheiro[a, b*], Claudomiro Vinicius Moreno Paschoa[a], Gledson Renan Salomão[a], Ianny Andrade Cruz[c], William Deodato Isique[a], Luiz Fernando Romanholo Ferreira[c], Farooq Sher[d], Nádia Hortense Torres[c], Vineet Kumar[e], Rafael Silvio Bonilha Pinheiro[a]

[a]School of Engineering, São Paulo State University (UNESP), Ave. Brasil Sul, number 56, ZIP Code 15385-000, Ilha Solteira - SP, Brazil.

[b]Brazil University, Street Carolina Fonseca, number 584, ZIP Code 08230-030, São Paulo – SP, Brazil.

[c]Graduate Program in Process Engineering, Tiradentes University, Ave. Murilo Dantas, number 300, ZIP Code 49032-490, Aracaju - SE, Brazil.

[d]Department of Engineering, School of Science and Technology, Nottingham Trent University, Nottingham NG11 8NS, United Kingdom.

[e]Department of Botany, School of Life Science, Guru Ghasidas Vishwavidyalaya, Koni, Bilaspur, Chattisgarh-495009, India.

* Corresponding author

E-mail addresses: americo.ju@gmail.com (J.H.P. Américo-Pinheiro)

Abstract

Every year, a considerable volume of medications is consumed. Because these medications are not entirely eliminated in the sewage treatment plants and impact the surface waterways, the environmental pollution problem arises. This study objective was to evaluate the possibility of using an absorbent material made with of polyethylene terephthalate and sugarcane bagasse ash functionalized with iron oxide (PETSCA/Fe^{3+}) in the removal of naproxen from water. The feasibility of having viable features in becoming an efficient adsorbent was first determined. The batch test was performed, allowing the dose effect, adsorption kinetics, and isotherm models to be evaluated. The determination of naproxen (NAP) concentration in water was analyzed on a high-performance liquid chromatograph and Langmuir method best represented the adsorption isotherm model. PETSCA/Fe^{3+} adsorbent material demonstrated potential in the naproxen removal at a low cost. The batching process was satisfactory, with 0.30 g of composite being the optimum fit for the system. The adsorption kinetics was determined and described by the pseudo second order model, with an average correlation coefficient (R^2) of 0.974. The adsorption system model was best represented by the Langmuir isotherm curve. Moreover, adsorption in the presence of H_2O_2 had a positive impact on the process, removing 81.9% of NAP, whereas the process without H_2O_2 did not remove more than 62.0% of NAP. Therefore, because of its good qualities for NAP removal, PETSCA/Fe^{3+} is recommended as adsorbent material, primarily in small-volume water filtration systems.

Keywords: Adsorption; anti-inflammatory; isotherm; water quality.

1. Introduction

Because non-steroidal anti-inflammatory drugs (NSAIDs) are widely acquired by the world population, their widespread detection in the environment is a major source of concern nowadays (Almeida et al., 2020). Since NSAIDs are not entirely digested by people or animals, they are discharged in the urine in conjugated or unmetabolized forms, reaching wastewater treatment plants. Nevertheless, traditional sewage treatment techniques are unable to effectively handle them, resulting in the release of these emerging contaminants (ECs) into water systems (Américo-Pinheiro et al., 2017; Ravi et al., 2020).

Although the concentrations of ECs in water are quite low, these contaminants can have negative impacts on ecosystems and human health after being acquired by organisms at different levels in the food chain (Cheng et al., 2021). Within this scenario, and given that water quality is considered a worldwide issue (Mian et al., 2021), the rising detection of these contaminants in water systems has generated concerns among researchers regarding water safety (Lin et al., 2020). As a result, the question of how to successfully remove ECs from water has also received considerable attention.

Environmental decontamination is difficult due to the limits of the procedures utilized for water and sewage remediation, such as the high cost and environmental concerns associated with real-time pollutant elimination (Rasheed et al., 2020). Thus, adsorption is a popular method for removing ECs since it is inexpensive to set up, extremely effective, of easy operation, and generally avoid the production of hazardous by-products (Rathi et al., 2021). Moreover, literature has shown that different adsorbents, such as activated carbons (Song et al., 2017), biochar (Ahmed et al., 2016), and graphene oxide (Hiew et al., 2019), are being utilized to remove ECs from water sources. However, many

commercial adsorbents can be very expensive (Pap et al., 2021), and that's the reason why the development and use of higher cost-benefit materials have been encouraged (Souza et al., 2021).

Among the most regularly used NSAIDs (i.e. diclofenac, ibuprofen, and paracetamol), naproxen has been regularly found in a variety of aquatic environments (i.e. marine, river, and drinking water) and even sediment (Tomul et al., 2020). Moreover, naproxen is a potential genotoxic agent that causes genotoxicity and oxidative stress, hence it must be removed from water bodies (Ahmad et al. 2018). As a result, as previously said, the adsorption procedure may be the ideal option due to its numerous comparative advantages.

Furthermore, in order to overcome the issue of expensive adsorbents, the by-products from agrobusiness and food processing industries may be exploited in the development of low-cost adsorbent materials (Souza et al., 2021). In this regard, Isique et al. (2017) developed a low-cost adsorbent from polyethylene terephthalate and sugarcane bagasse ash functionalized with iron oxide (PETSCA/Fe^{3+}); and this material was previously used to remove diclofenac by Salomão et al. (2021) with satisfactory results.

In this study, the adsorption of naproxen from supply water by PETSCA/Fe^{3+} is evaluated by batch experiments. Additionally, the naproxen dosage effect, adsorption kinetics, and isotherm models were analyzed and discussed.

2. Methodology

The adsorbent used in this study was prepared from polyethylene terephthalate supplied by a plastic industry and sugarcane bagasse ash calcined from an ethanol distillery boiler. The materials were sieved to obtain homogeneous particles (0.85 μm)

according to the methodology proposed by Isique et al. (2017). The preparation of the PETSCA/Fe^{3+} adsorbent was carried out by precipitating iron oxides formed by dropping sodium hydroxide (5.0 M) into an aqueous suspension containing activated PETSCA and $FeSO_4.7H_2O$ (14 mmol) at 70 °C. The material obtained was filtered, washed with deionized water and then dried in an oven at 60 °C for 24 h (Isique et al., 2017).

The adsorbent PETSCA/Fe^{3+} was investigated to determine if it had any viable features for being an effective adsorbent. When the viability of the material was confirmed, the batch test was performed, thus allowing the assessment of the dosage effect, adsorption kinetics, and the isotherm models.

2.1. Preparation of solution samples containing naproxen

Naproxen solution (97.0% pure, Nanjing Dorra Pharmaceutical Technology Cg. Ltd/ - China) at a concentration of 2.51 g L^{-1} was diluted in deionized water to simulate supply water contaminated with the anti-inflammatory, resulting in a working solution of 1,000 µg L^{-1}. The naproxen concentration analyzed in the research was selected according to the revised literature (Salomão et al., 2021).

2.2.PETSCA/Fe^{3+} composite physicochemical characterization

The PETSCA/Fe^{3+} adsorbent was developed and evaluated according to the study by Isique et al. (2017). The physicochemical characteristics of the composite were verified by means of X-ray diffraction Fourier Transform Infrared Spectroscopy (FTIR), Scanning Electron Microscope (SEM) analysis, X-ray energy dispersive spectroscopy (EDX) and

density. However, this research was based on repeating the SEM and density assessments, as they were the most important characteristics for the development of the study.

2.2.1. SEM

The porosity evaluation of the PETSCA/Fe^{3+} composite is necessary to determine the adsorbent surface, because adsorption is a surface phenomenon and its intensity depends on the specific surface area (Isique et al., 2017). Thus, a sample of the composite was taken to the laboratory and analyzed by SEM (model Zeiss EVO LS15), with a magnification capacity of up to 20,000 times.

2.2.2. Adsorbent density characterization

Bulk density was calculated by removing a previously defined dry mass volume of PETSCA/Fe^{3+} adsorbent, placing it in a container of known mass on extreme precision.

Deionized water was used to fill the container and the weighing was repeated. Following these procedures, the calculations to obtain the PETSCA/Fe^{3+} adsorbent density were obtained.

2.2.3. Point of zero charge (pH PZC)

The pH PZC is a critical metric for determining the adsorbent material's viability and efficacy in relation to the compound's surface load (positive or negative). This parameter is defined by the composite surface's null pH value, which occurs when positive and negative surface loads are equivalent.

The test was carried using the "experiment of the 11 points". In the pHPZC analysis, 0.30 g of the adsorbent was added to 25 mL of 0.1 M aqueous NaCl solution and adjusted

with 0.1 M HCl or NaOH solutions at 12 distinct initial pH settings (2, 3, 4, 5, 6, 7, 8, 9, 10, 11, 12, 13). Preparation was done on the solutions and the final pH of the solution was obtained after 24 h of shaking at 150 rpm at 25 ^{o}C on an orbital shaker table (Deltalab) to maintain equilibrium in a thermostatic bath.

2.3. PETSCA/Fe^{3+} mass determination for NAP adsorption in deionized water

The sampling was based on separating 6 masses of PETSCA/Fe^{3+} (0.05, 0.10, 0.20, 0.30,0.40, and 0.50 g), and inserting them in Erlenmeyer flasks with a 25 mL working solution containing naproxen at a concentration of 1,000 µg L^{-1}. Moreover, the samples were evaluated in the hydrogen peroxide (500 µL) presence and absence at pH 7.0.

In order to find the mass of PETSCA/Fe^{3+} that would allow for higher adsorption, the assays were done in triplicate and, as a result, more removal of naproxen from the water supply. The erlenmeyers were placed on the orbital shaker (Deltalab) and stirred at 150 rpm for 24 h at a temperature of 25 ^{o}C. Subsequently, these solutions were extracted, prepared and sent for chromatographic analysis.

2.4. Adsorption kinetic study

The purpose of this research was to determine when naproxen and the PETSCA/Fe^{3+} surface are in adsorption equilibrium, that is, when the adsorption and desorption processes in the system occurred equally and simultaneously. In this assay, the mass of the PETSCA/Fe^{3+} adsorbent determined in the prior analysis (item 2.3) was used, with only the contact time changing (5 to 180 min). The adsorbent material was added in seven 125 mL Erlenmeyer, each with 25 mL of naproxen working solution (1,000 µg L^{-1}) at

room temperature (25 to 30 °C) and pH ~ 7.0. The experiment was performed in the same way, but with the addition of 500 µL of H_2O_2. The samples were taken to the agitator table and agitated at 150 rpm. The analysis was performed for three different temperatures (25, 35 and 45 ^oC) in order to evaluate the effect of temperature over time. The samples were extracted by the dispersive liquid-liquid microextraction (DLLME) method and prepared for analysis by chromatography, always at the end of each stirring interval. At each time investigated, the adsorption capacity (qt) was obtained.

2.5. Adsorption isotherm study

For the isotherm tests, the adsorbent mass obtained in the mass determination assay was employed, differentiating only the concentration of the naproxen working solution, which in this analysis was not constant. This concentration ranged from 31.25 to 1,000 µg L^{-1} at pH ~ 7.0 for a period of 24 h under agitation of 150 rpm at room temperature (25 to 30 °C). After shaking, the samples were subjected to centrifugation and the final concentrations were extracted, filtered and suitable for chromatographic analysis.

The experiment was repeated with the addition of H_2O_2 (500 µL) under the same conditions as before, except at room temperature (25 to 30 °C), because the effects of the adsorption process were observed placing temperatures at 25, 35 and 45 ^oC. The Langmuir and Freundlich equations were used to calculate the adsorbed amounts per mass unit under equilibrium conditions (Nascimento et al., 2020).

To calibrate the experimental results, the Langmuir and Freundlich isotherm models were applied (Freundlich, 1906; Langmuir, 1917). The Langmuir model equation is one of the most commonly used to model adsorption processes, according to Nascimento et al. (2020). From this equation, the following assumptions are made: (i) there is a defined

number of sites; (ii) the sites have equal energy and there is no interaction between the adsorbed molecules; (iii) the adsorption takes place on a monolayer; and, (iv) each site can have only one adsorbed molecule.

Nascimento et al. (2020) state that efficient adsorbents have high q_{max} and K_L values. The K_L constant is associated with the free energy of adsorption, which refers to the affinity between the surface of the adsorbent and the adsorbate. Briefly, these parameters efficiently indicate the nature of the adsorbent, where R_L denotes that isotherm is said unfavorable when ($R_L>1$), linear ($R_L=1$), and favorable ($0<R_L<1$) or irreversible ($R_L=0$).

2.6. Naproxen chromatographic analysis and DLLME

The microextraction step is one of the most important elements of the sampling process, given the difficulty of separating the sample's organic phase. First, both the samples of the water supply solution with NAP (1,000 g L^{-1}) and the final analyses taken from the adsorption process (5.0 mL) were filtered and transferred to 15.0 mL Falcon-type conical tubes. All Falcon tubes containing organic material had their procedures realized according to the method suggested by Moreira et al. (2014). In this experiment, 500 µL of methanol (HPLC grade) was used as a dispersing agent, combined with 500 µL of carbon tetrachloride (HPLC grade) as an extracting agent. These agents (disperser and extractor) are responsible for separating and synthesizing only the organic phase of the sample so that it is later centrifuged and completely separated from the aqueous phase. Then, the organic phase of each tube was extracted with a micro syringe and deposited in 10.0 mL test tubes, and these were taken to a stove, where drying occurred under the gaseous nitrogen flow. Before being taken to the chromatograph for detection and quantification, the samples were in 300 µL of methanol (HPLC grade), and subsequently,

20 µL of the analyte was insert into a liquid chromatograph with high performance. The chromatography equipment used in this experiment was a high-efficiency liquid chromatograph (Shimadzu). The chromatograph was integrated with a CBM-20A, two LC-20AT pumps, a Rheodyne Injector (Rohnert Park, CA, USA) with a 20 µL loop valve, and a diode array detector (SPD-M20A), wavelengths from 220 nm to 280 nm and LCsolution software for detection and quantification of NAP samples. Organic solvents HPLC grade used were acetonitrile, trifluoroacetic acid, carbon tetrachloride, methanol, acetone, and aqueous solvent ultra-filtered water. LC Column Shim-pack C18 (250 mm x 4.6 mm ID, 5.0 m particles) chromatographic columns were employed. For better data validation, the sample injection in HPLC was repeated for three times in a sample volume of 20.0 µL.

The validation of the methodology used to quantify the NAP in the tested solution was performed using the drug's analytical curve. The curve was made using the detection limits (DL: 0.0009 µg L^{-1}) and quantification (QL: 0.0026 µg L^{-1}) of the NAP.

3. Results and Discussion

3.1. Characterization of the PETSCA/Fe^{3+}

Initially, a verification was carried out in order to validate the material and analyze whether the composite has any adsorbent characteristics. When SEM was employed to examine its structure, it was noticed that the substance, polyethylene terephthalate , had fused with sugarcane bagasse ash, proving which was presented by Isique et al. (2017). The surface structure of the adsorbent can be seen in Fig. 1a.

The iron mineral (melanterite) was also found, since PET + SCA + iron is the same compound, the PETSCA/Fe^{3+} was characterized, and it was possible to observe an adsorbent with irregular area, suggesting that it may have higher efficiency through physical adsorption processes.

The point of zero charge (pH PZC) is a relevant factor for adsorption efficiency of the composite. This property was evidenced because it allowed the adsorbent's surface charge to be predicted. The pH PZC value for the adsorbent (Fig. 1b) was 4.5, which shows the behavior of the reactions in the aqueous solution. At a solution pH near to 7.0 (higher than PZC pH), it is believed that the solid surface charge is negatively charged, which is beneficial for the positive charge molecule adsorption, indicating that the adsorption of naproxen in water is promising.

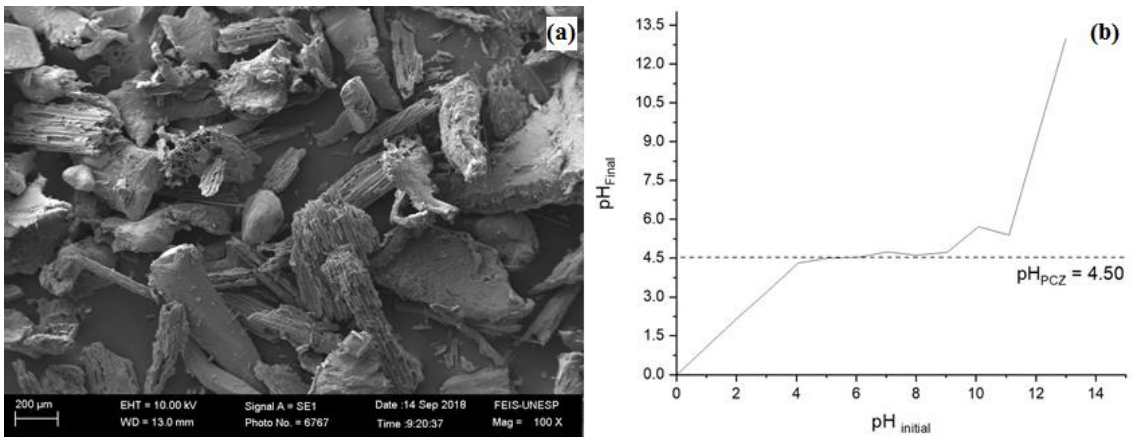

Fig. 1. (a) Surface structure of the adsorbent and (b) point of zero charge of PETSCA/Fe^{3+}

Kurtulbaş et al. (2017) evaluated 3 distinct Amberlite resins (XAD-2, XAD-4, and XAD-16) for the NAP adsorption. They prepared acidic and basic working solutions, with the acidic solutions yielding better results. At pH 3.0, XAD-4 adsorbed 99.7% of NAP. When pH < pKa, NAP behaved as a neutral molecule and non-electrostatic interactions occurred on the surface. The NAP pK is 4.15, and at acidic pH values, the adsorption

process depends on non-electrostatic interactions. At pH values > 4.15, NAP was negatively charged. Furthermore, the resin surfaces were negatively charged. Thus, the adsorption capacities of the adsorbents were lower at basic pH values.

3.2. PETSCA/Fe^{3+} mass measurements

Table 1 shows that a mass of 0.5 g has a removal rate of less than 0.3 g. Thus, even if the amount of adsorbent mass is increased, there is no proportionality relationship with the increase in NAP removal. The overlapping or aggregation of active sites during the interaction process between adsorbate and adsorbent might induce a decrease in the overall surface area accessible for adsorption, which can explain this behavior (Garg et al., 2004; Huang et al., 2011).

In a study that investigated the effect of the dosage of an adsorbent consisting of Cu-doped Mil-101 (Fe) for adsorption of NAP and ibuprofen, it was possible to observe that the drug removal rates reached the maximum when the amount of adsorbent was 10 mg and that the increase in the amount of adsorbent was not able to improve the adsorption rates of anti-inflammatory drugs (Xiong et al., 2021).

Table 1: Adsorption capability and naproxen removal % in aqueous medium as a function of PETSCA/Fe^{3+} dose

Samples	Mass (PETSCAFe^{3+}) (g)	Volume (L)	C_e (µg L^{-1})	q_e (µg g^{-1})	Removal (%)
Control			**1191.157**		
1	0.0520	0.025	867.187	416.917	27.2
2	0.1029	0.025	567.100	137.779	52.4
3	0.2015	0.025	13.711	1.701	98.8

4	0.3035	0.025	2.086	0.172	99.8
5	0.4003	0.025	5.135	0.321	99.6
6	0.5008	0.025	50.136	2.503	95.8

Ce: naproxen concentration at equilibrium; qe: adsorption capacity

Salomão et al. (2021) performed a mass determination test for sodium diclofenac (DIC) adsorption using the PETSCA/Fe^{3+} composite, and obtained a result similar to this study, with 0.3 g of mass reaching the greatest removal rate under the same conditions. Nevertheless, according to Nodeh et al. (2021), NAP removal evolved considerably as the dosage of magnetic graphene oxide composite functionalized with hybrid silica gel was increased from 5 to 30 mg, becoming constant from this mass.

Rafati et al. (2016) discovered that increasing the adsorbent dose from 0.125 to 1 g L^{-1} increased the highest adsorption efficiency from 78.4 to 92.2%, since the adsorbent amount increases the number of active adsorption sites on the adsorbent available for naproxen ions. Additionally, a study evaluating NAP removal using Amberlite XAD-4 resin concluded that the maximum removal percentage (99.8%) was obtained with 0.5 g of adsorbent (Kurtulbaş et al., 2017).

3.3. Adsorption kinetics

In water treatment systems that use the adsorption process, it is of fundamental importance to investigate the contact time between the adsorbent and adsorbate in the solution, in this case PETSCA/Fe^{3+} and NAP, respectively. This analysis allows us to identify the time it takes for mass transfer to begin, i.e., NAP adsorption by the PETSCA/Fe^{3+} composite, as well as the time it takes for the system to reach equilibrium and no more adsorption occurs. On a real scale, this parameter would be used to evaluate

the time of containment of the water supply in the reservoir to occur the effective adsorption, and the time that the adsorbent should be replaced. The mathematical models that were used in this study for the determination of kinetics are those of pseudo-first order, pseudo-second order, and intraparticle diffusion.

At first, data for the kinetic model's curve was collected and calculated at room temperature (25 to 30 °C) with absence of H_2O_2 (Table 2). Then, the data on contact time and percentage of removal over time and temperatures of 25, 35, and 45 ^oC with the addition of H_2O_2 allowed the assessment of the influence that this substance would cause on the mass transfer reaction. Table 2 shows the amount of NAP that was adsorbed by the PETSCA/Fe^{3+} composite until it reached balance (adsorption/desorption). The adsorption process had a total duration of 180 min, ranging from 5 to 180 min.

Table 2: Removal and adsorption of naproxen in water in a kinetic reaction at room temperature (25 to 30 °C) absent H_2O_2 and at 25, 35 , and 45 ^oC with the inclusion of H_2O_2

Adsorption kinetics – Room temperature (25 to 30 °C) - Without H_2O_2						
Sample	**Contact time (min)**	**Volume (L)**	**Mass (g)**	**Ce (µg L^{-1})**	**qe (µg g^{-1})**	**Removal (%)**
Control		0.025	no mass	934.592		
1	5	0.025	0.3003	760.915	22.454	26.2
2	15	0.025	0.3006	445.977	48.624	56.7
3	30	0.025	0.3003	352.247	56.476	65.8
4	45	0.025	0.3005	271.516	63.154	68.6
5	60	0.025	0.3003	288.632	61.772	71.9
6	120	0.025	0.3007	379.241	54.156	73.2
7	180	0.025	0.3002	127.508	75.210	87.6
Adsorption kinetic – Temperature 25 ^oC - With H_2O_2						

Sample	Contact time (min)	Volume (L)	Mass (g)	Ce (µg L^{-1})	qe (µg g^{-1})	Removal (%)
Control		0.025	no mass	1078.404		
1	5	0.025	0.3003	858.995	18.265	20.3
2	15	0.025	0.3006	464.287	51.074	56.9
3	30	0.025	0.3003	330.781	62.239	69.3
4	45	0.025	0.3005	259.891	68.095	75.9
5	60	0.025	0.3003	176.075	75.118	83.7
6	120	0.025	0.3007	99.266	81.404	90.8
7	180	0.025	0.3002	84.646	82.758	92.2

Adsorption kinetic - Temperature 35 °C - With H_2O_2

Sample	Contact time (min)	Volume (L)	Mass (g)	Ce (µg L^{-1})	qe (µg g^{-1})	Removal (%)
Control		0.025	no mass	1084.199		
1	5	0.025	0.3009	799.766	23.631	26.2
2	15	0.025	0.3006	712.348	30.925	34.3
3	30	0.025	0.3008	356.437	60.485	67.1
4	45	0.025	0.3009	281.607	66.682	74.0
5	60	0.025	0.3000	313.682	64.209	71.1
6	120	0.025	0.3007	108.056	81.155	90.0
7	180	0.025	0.3003	80.527	83.555	92.6

Adsorption kinetic - Temperature 45 °C - With H_2O_2

Sample	Contact time (min)	Volume (L)	Mass (g)	Ce (µg L^{-1})	qe (µg g^{-1})	Removal (%)
Control		0.025	no mass	1030.639		
1	5	0.025	0.3006	863.042	13.938	16.3
2	15	0.025	0.3009	684.784	28.735	33.6

3	30	0.025	0.3005	541.970	40.654	47.4
4	45	0.025	0.3000	424.029	50.550	58.8
5	60	0.025	0.3003	375.069	54.576	63.6
6	120	0.025	0.3002	197.310	69.397	80.9
7	180	0.025	0.3008	67.939	80.0111	93.4

Ce: naproxen concentration at equilibrium; qe: adsorption capacity

The PETSCA/Fe^{3+} adsorption process in interaction with the aqueous solution is instantaneous, since there is an adsorption of more than 15.0% naproxen in all samples during the first 5 min.

The results with temperature at 45 ºC show an increase in removal efficiency over time, since at the end more than 93.0% of naproxen removal was obtained. However, it is based on the fact that there is a reduction in drug removal in the initial time of 5 min, which is around 16.2%, when compared to data of 25 and 35 ºC.

According to Nascimento et al. (2020), as the temperature rises, there is a loss of viscosity in the solution as well as dilatation of the pores of the adsorbent material, which increases the adsorption area of the adsorbent material.

The adsorbent was in contact with the adsorbate for 180 min, and the system began to lower the percentage of removal after 120 min, becoming stable, and reaching complete stability in 180 minutes. Thus, it is observed that the physical-chemical interactions responsible for adsorption and desorption remained balanced and there was no further removal of the drug. It should also be noted that even without H_2O_2, the adsorption process reached equilibrium in 180 min (Table 2).

In a study employing graphene oxide functionalized with hybrid silica gel as an adsorbent composite in NAP adsorption, the authors obtained a contact time of 90 min, from which it was possible to achieve adsorption equilibrium (Nodeh et al., 2021).

Salomão et al. (2021) in their study on diclofenac adsorption using PETSCA/Fe^{3+} composite, obtained an initial rate in the first 5 min ranging from 20 to 48.0% of DIC removal at a temperature of 25, 35, and 45 ^{o}C, with and without H_2O_2.

Phasuphan et al. (2019) used chitosan-modified tire rubber to test the adsorption reaction rate of NAP and found that the adsorption effectiveness of the modified adsorbent steadily rose during the first 2 h before becoming basically steady. The fast adsorption during the first period may be attributed to the large number of active sites on the chitosan-modified adsorbent surface, as well as a high affinity for NAP. The time it took for NAP adsorption to reach equilibrium was around 2 h, during which time about half of the NAP was removed.

The adsorption speed of textile dyes in montmorillonite particles was studied by Kamranifar and Naghizadeh (2017), who found that the most adsorption happened in the first 15 min, and that this period was excellent for the adsorption process.

In another study, Fenton's reaction had as main role to make the adsorption reaction more stable and gradual in relation to time, but it is noted that even without the addition of H_2O_2, the process occurred satisfactorily reaching the end of the contact time 87.6% of removal. The Fenton reaction's consistency can be ascribed to the connection that occurs when Fe^{3+} and H_2O_2 contact, creating hydroxyl radicals that aid in adsorption gradation (Salomão et al., 2021).

Regarding the model that best describes the adsorption kinetics process, another parameter that expresses the modeling of the data is the correlation coefficient (R^2). In this case, the closer this coefficient is to 1, the more straight the line is and the more likely this event will occur largely in the solution (Table 3).

Table 3: Coefficient of kinetic models in the process of adsorption naproxen in aqueous solution using PETSCA/Fe^{3+} based on the temperatures and presence of H_2O_2

	Correlation coefficient (R^2)			
H_2O_2	**Temperature (°C)**	**Intraparticle diffusion**	**Pseudo-first order**	**Pseudo-second order**
Presence	25	0.8192	0.1947	0.9931
Presence	35	0.8864	0.0933	0.9825
Presence	45	0.9249	0.0001	0.9645
Absent	Room temperature (25 to 30)	0.7193	0.0715	0.9564

When the temperature was elevated to 45 ºC, reactions involving intraparticle diffusion became more relevant, but the pseudo-second order R^2 appeared to be considerably closer to 1 at all temperatures, with and without the addition of H_2O_2. It is also possible to see that pseudo-second order process had greater R^2, which could be related to chemical reactions (chemisorption) occurring in the process, which continued to grow with the increase in temperature. Regardless of whether H_2O_2 was supplied or not, the determination coefficient results from the analysis without H_2O_2 demonstrated that the process tended to happen by pseudo-second-order model.

Similarly, Nodeh et al. (2021) obtained a kinetic curve modeling focused on the pseudo-second order model (PSO) with a R^2 equal to 0.998 when analyzing the kinetic process of NAP adsorption in contact with adsorbent based on magnetic graphene oxide functionalized with hybrid silica gel. Salomão et al. (2021) used the PETSCA/Fe^{3+} composite to evaluate the adsorption kinetics process in DIC removal, and came up with a pseudo-second order model with a correlation coefficient of over 96.0%.

Rafati et al. (2016) demonstrated that naproxen adsorption utilizing a nano-clay-based composite has a beneficial effect, with the Ellovich kinetic model best fitting the

adsorption process. Tomul et al. (2020) prepared a composite from different carbonization processes of peanut-derived biochar for testing in NAP adsorption, and concluded that the adsorption kinetics model that best fit the study was the pseudo-second order (PSO) in comparison with pseudo-first order (PPO) and Ellovich models, and the adsorption kinetics reached a fast equilibrium (<120 min).

The results of a NAP adsorption investigation employing residual rubber from tires treated with chitosan as an adsorbent were also reported using the pseudo-second order kinetic model. As a result, the adsorption capacity of the adsorbent was proportional to the number of active sites on the surface, and chemisorption was the rate-limiting stage of the process (Ho & McKay, 1999; Hong et al., 2014; Phasuphan et al., 2019).

Vieira, Becegato and Paulino (2021) evaluated the effect of adsorption kinetics on the removal of 2,4-dichlorophenoxyacetic acid in chitosan-based hydrogel adsorbent and concluded that the best kinetic fit was found with the pseudo-second order kinetic model, according to the highest R^2. Smiljanic et al. (2021) observed the characteristics of the adsorption kinetics of zeolite composite in the removal of NAP, and concluded that the pseudo-second order model is the most common way to describe the process, but only for the sake of simplicity of the method, because the pseudo-first order model also produced satisfactory results.

3.4. Adsorption isotherm

The results obtained with adsorption isotherm data are extremely important to actually evaluate the real ability of PETSCA/Fe^{3+} to remove NAP from the water by performing a graphic modeling, tracing the two models of isotherm curves (Langmuir and Freundlich) and comparing the data.

411 Table 4 presents the values of naproxen concentration (% and µg L^{-1}), Ce, qe and NAP
412 removal rate (%) at room temperature (25 to 30 °C), without addition of H_2O_2, and with
413 the addition of H_2O_2 at 25, 35 and 45 ^oC.
414
415 **Table 4:** Isotherm data obtained using PETSCA/Fe^{3+} at room temperature (25 to 30 °C) absent
416 H_2O_2 and at different temperatures with the inclusion of H_2O_2 in the adsorption of naproxen in
417 supply water.

Isotherm room temperature (25 to 30 °C) without H_2O_2						
Sample	**Concentration (%)**	**Mass (g)**	**Concentration (µg L^{-1})**	**Ce (µg L^{-1})**	**qe (µg g^{-1})**	**Removal (%)**
Control		No mass	1081.7			
1	3.125	0.300	16.9	9.637	0.619	57.0
2	6.25	0.300	33.8	20.852	1.093	61.7
3	12.5	0.300	67.6	25.666	3.580	37.9
4	25	0.300	135.2	81.864	4.572	60.5
5	50	0.300	270.4	157.835	9.693	58.4
6	100	0.300	540.9	278.683	22.233	51.5
Isotherm at 25 ºC with H_2O_2						
Sample	**Concentration (%)**	**Mass (g)**	**Concentration (µg L^{-1})**	**Ce (µg L^{-1})**	**qe (µg g^{-1})**	**Removal (%)**
Control		No mass	1020.8			
1	3.125	0.300	16.0	10.315	0.480	64.7
2	6.25	0.300	31.9	20.014	1.003	62.7
3	12.5	0.300	63.8	26.450	3.188	41.5
4	25	0.300	127.6	83.362	3.791	65.3
5	50	0.300	255.2	159.190	8.266	62.4
6	100	0.300	510.4	341.086	14.359	66.8

Isotherm at 35 ºC with H_2O_2						
Sample	**Concentration (%)**	**Mass (g)**	**Concentration (µg L^{-1})**	**Ce (µg L^{-1})**	**qe (µg g^{-1})**	**Removal (%)**
Control		No mass	1060.3			
1	3.125	0.300	16.6	13.221	0.289	79.8
2	6.25	0.300	33.1	25.773	0.634	77.8
3	12.5	0.300	66.3	35.151	2.693	53.0
4	25	0.300	132.5	108.359	2.091	81.7
5	50	0.300	265.1	211.038	4.676	79.6
6	100	0.300	530.2	434.423	8.295	81.9

Isotherm at 45 ºC with H_2O_2						
Sample	**Concentration (%)**	**Mass (g)**	**Concentration (µg L^{-1})**	**Ce (µg L^{-1})**	**qe (µg g^{-1})**	**Removal (%)**
Control		No mass	1007.4			
1	3.125	0.300	15.7	8.995	0.583	57.2
2	6.25	0.300	31.5	21.458	0.867	68.2
3	12.5	0.300	63.0	35.329	2.392	56.1
4	25	0.300	125.9	92.080	2.928	73.1
5	50	0.300	251.9	192.014	5.169	76.2
6	100	0.300	503.7	397.908	9.136	79.0

Ce: naproxen concentration at equilibrium; qe: adsorption capacity

In a superficial examination of the data, it has been noted that the isotherm with the lowest final removal percentage was that of the samples done at room temperature (25 to 30 °C) without H_2O_2, that have reached a maximum of 61.7%. On the other hand, the isotherm that presented the best removal data (81.9%) was the isotherm with H_2O_2 at 35 ºC.

Thus, Fenton reaction throughout the process prevailed, as adsorption of adsorbent material without H_2O_2 addition did not achieve removal rates above 62.0% during the assay. The results were graphically presented according to the isotherm curves explored in this work, Langmuir and Freundlich, to better illustrate the data shown in Table 4. Fig. 2a shows the Langmuir isotherm curves for NAP adsorption on PETSCA/Fe^{3+} at the three temperatures (25, 35 and 45 ^{o}C), as well as at room temperature (25 to 30 °C), without adding H_2O_2 (Fig. 2b). Similarly, Fig. 2c presents the Freundlich model's isotherm adjustment.

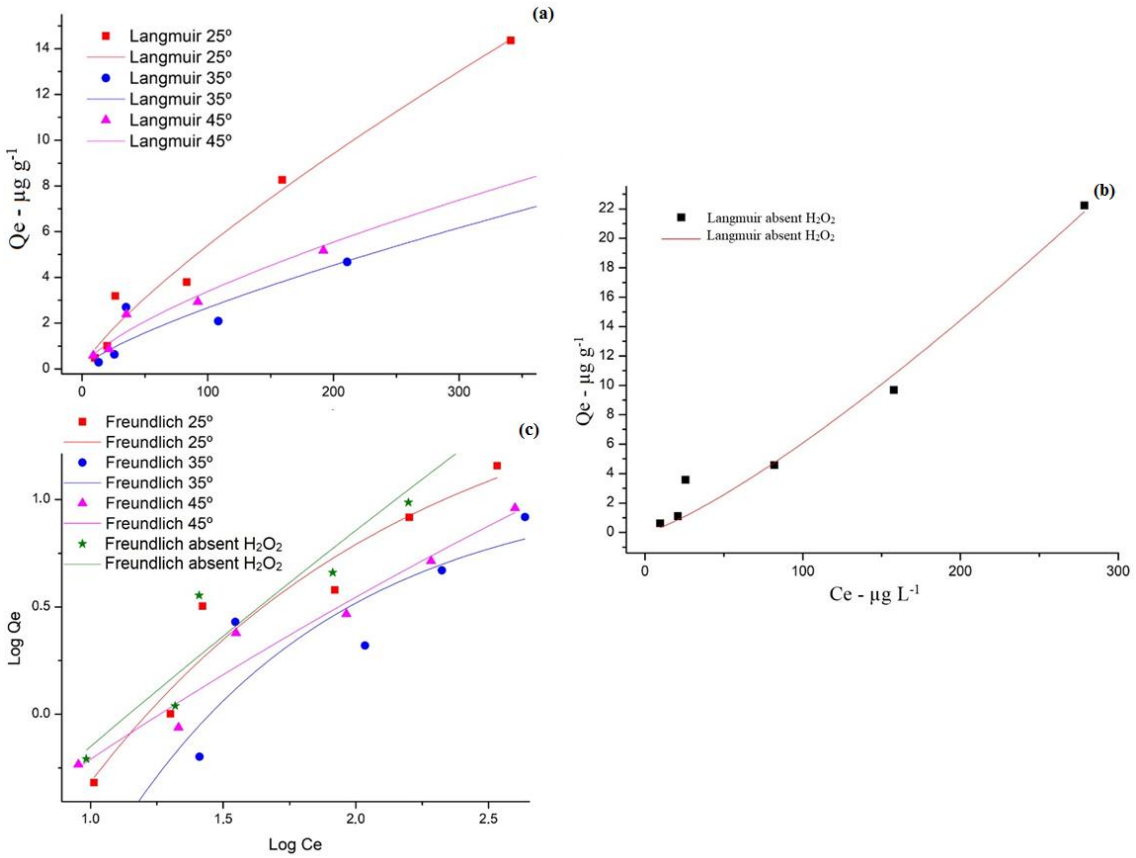

Fig. 2. (a) Naproxen adsorption isotherms in solution simulating supply water, through the adsorbent PETSCA/Fe^{3+}, and Langmuir adjustment curves for 25, 35, and 45 ^{o}C temperatures, (b) naproxen adsorption isotherms in solution simulating supply water, through the adsorbent PETSCA/Fe3+, and Langmuir adjustment curves for room temperature (25 to 30 °C) without H_2O_2 addition and (c) Naproxen

adsorption isotherms in solution simulating supply water, through the adsorbent PETSCA/Fe^{3+},and Freundlich adjustment curves for 25, 35, 45 ºC and room temperature (25 to 30 °C)

According to the graphical data (Fig. 2a, b, c), it is observed that both models fit the results well, the two models are within the linear and satisfactory classification, since the concavity of the curve is facing down.

The Langmuir model was assumed to be the best fit curve for NAP adsorption on PETSCA/Fe^{3+} using isotherm curve modeling. Because the mass of retained adsorbate (qe) per unit mass of the adsorbent is large for a low equilibrium concentration of the adsorbate in the liquid phase (Ce), Langmuir is beneficial, as can be seen from its concavity (Moreira, 2008).

Regardless the curve concavity allows the Langmuir model to be accepted as favorable, there is a need to confirm this positive variation with the certification parameters, like R^2 and the constants of each model considered here KL (Langmuir) and KF (Freundlich) to obtain higher reliability of the results. Table 5 illustrates each parameter addressed according to the model presented.

Table 5: Parameters of the Langmuir and Freundlich models of the adsorption isotherms of naproxen in aqueous solution simulating supply water using PETSCA/Fe^{3+} as adsorbent, at different temperatures

Model	**Parameter/ Temperature (°C)**	**25**	**35**	**45**	**Room temperature (25 to 30 °C) absent H_2O_2**
Langmuir	qmax (mg g^{-1})	26.5245	34.9238	40.6666	-4.2141
	KL (L mg^{-1})	0.0305	0.0197	0.0210	0.0761
	R^2	0.9709	0.9215	0.9689	0.9656
Freundlich	KF (mg g^{-1})	0.3230	0.2865	0.3867	0.3241

$(L\ mg^{-1})^{1/n}$)				
N	3.3444	3.5335	4.0650	1.0128
R^2	0.9149	0.8241	0.9242	0.9269

458

459 The R^2 for the Langmuir and Freundlich isotherms demonstrate that the Langmuir
460 model is more efficient than the Freundlich model in terms of adsorption results
461 correlation, as it has an R^2 closer to 1 at all tested temperatures (25, 35 and 45 °C).
462 When assessing the influence of 2,4-dichlorophenoxyacetic acid adsorption isotherm
463 on chitosan-based hydrogel adsorbent, Vieira, Becegato, and Paulino (2021) found that
464 the Sips curve best fit the process because it had the best R^2 among the tested models
465 (Langmuir, Freundlich, Redlich-Peterson and Sips).
466 Batch adsorption experiments with NAP and ibuprofen in water using Cu-doped Mil-
467 101 (Fe) as adsorbent material indicated a good fit of the pseudo-second order kinetic
468 model suggesting a chemical adsorption of these anti-inflammatory drugs (Xiong et al.,
469 2021). The Langmuir model was the one that best represented the adsorption isotherms
470 of the evaluated contaminants, showing that the adsorption of drugs occurs in monolayers
471 (Xiong et al., 2021). Thus, the results of the aforementioned study with Cu-doped Mil-
472 101(Fe) corroborate the results obtained in our research with the PETSCA/Fe^{3+} adsorbent
473 aimed at removing NAP from water.
474 Tomul et al. (2020) evaluated the adsorption isotherm models using working solutions
475 prepared from a stock solution of naproxen with a concentration of 1,000 mg L^{-1}. In a 250
476 mL solution with a target concentration of naproxen, 0.125 g of each type of biochar
477 composite was added. The Langmuir model may therefore effectively describe the
478 experimental data based on the R^2 (Tomul et al., 2020).
479 According to Nascimento et al. (2020), a favorable adsorption has a RL value ranging
480 from 0 to 1 in the Langmuir model, indicating that adsorbate prefers the solid phase to

the liquid phase and that the adsorption is favorable. The application of the RL factor to the Langmuir isotherm yields a value of 0.012 for room temperature (25 to 30 °C) without H_2O_2, 0.031 for a temperature of 25 °C, 0.045 for 35 °C, and 0.045 for 45 °C. So this number is smaller than one shows that the isotherms in the concentration levels under consideration are favorable.

Through the analysis of the 1/n empirical parameter of the Freundlich isotherm, it was found that the parameter presented a value of 0.299 for the temperature of 25 °C, 0.283 for 35 °C, 0.26 for 45 °C, and 0.9873 for room temperature (25 to 30 °C) without H_2O_2. All of the values were below 1, showing that the adsorption process favored Freundlich; nevertheless, because Langmuir's determination coefficient was higher, it won out.

Based on the results of Nodeh et al. (2021), the adsorption process developed in their study was well adjusted to the Langmuir model due to a good R^2 (0.99), elucidating that the adsorption system occurs via a monolayer for naproxen adsorption on the surface of the compound of graphene oxide functionalized with hybrid silica gel.

According to the data obtained by Feng et al. (2021) in their research on NAP adsorption in adsorbent material based on reduced graphene oxide and immobilized with β-cyclodextrin, the authors observed that the best modeling of the isotherm curve was obtained by Langmuir isotherm, with values of 1/L lower than 0, indicating favorable adsorption curves.

The Langmuir isotherm model represented the DIC adsorption best when PETSCA/Fe^{3+} was used as the adsorbent material. In this study, the adsorbent material to remove more than 96.0% of DIC (Salomão et al., 2021).

Another study used three types of Amberlite resin (XAD-2, XAD-4, and XAD-16) to test the adsorption isotherm model for NAP adsorption, and found that the adsorption

follows the Langmuir process, occurring in a monolayer and obtaining a R_L coefficient between 0 and 1 in all samples (Kurtulbaş et al., 2017).

The isotherm model that best fit the study with the chitosan-modified fragmented rubber tire adsorbent, in NAP adsorption, was the Freundlich isothermal model with correlation coefficient of 0.9863 (Phasuphan et al., 2019). Thus, NAP removal by rubber can be attributed to multilayer adsorption on the heterogeneous surface, which differs from the PETSCA/Fe^{3+} adsorbent that occurs by the Langmuir isotherm model.

Smiljanic et al. (2021) studied zeolite-rich composites as adsorbent material in NAP adsorption from water, and also observed that the Langmuir isotherm best fit the adsorption process, with an adsorption capacity (qmax) of 16.1 mg of NAP per gram of adsorbent in buffer solution.

4. Conclusion

The adsorbent material PETSCA/Fe^{3+} has potential in the naproxen removal process. In a batch adsorption process with H_2O_2, PETSCA/Fe^{3+} demonstrated the removal of naproxen. Adsorption in the presence of H_2O_2 had a positive impact on the process, removing 81.9% of the NAP, while the process without H_2O_2 did not remove more than 62% of the NAP. In the aqueous medium, kinetics was achieved through a pseudo-second order reaction, which restricted adsorption to chemisorption processes. The Langmuir isotherm curve model best described the adsorption system, which characterizes a process occurring in monolayers.

We recommend PETSCA/Fe^{3+} as an adsorbent material for naproxen removal in small volume water filtration systems. The product is viable because, in addition to its ability to remove the anti-inflammatory, it has a low cost to produce.

References

Ahmad, M.H., Fatima, M., Hossain, M., Mondal, A.C., 2018. Evaluation of naproxen-induced oxidative stress, hepatotoxicity and in-vivo genotoxicity in male Wistar rats. J. Pharm. Anal. 8, 400-406. https://doi: 10.1016/j.jpha.2018.04.002.

Ahmed, M.B., Zhou, J.L., Ngo, H.H., Guo, W., CHEN, M., 2016. Progress in the preparation and application of modified biochar for improved contaminant removal from water and wastewater. Bioresource. Technol. 214, 836–851. https://doi.org/10.1016/j.biortech.2016.05.057.

Almeida, H.F.D., Neves, M.C., Trindade, T., Marrucho, I.M., Freire, M.G., 2020. Supported ionic liquids as efficient materials to remove non-steroidal anti-inflammatory drugs from aqueous media. Chem. Eng. J. 381, 122616. https://doi.org/10.1016/j.cej.2019.122616.

Américo-Pinheiro, J.H.P., Isique, W.D., Torres, N.H., Machado, A.A., Carvalho, S.L., Valério Filho, W.V., Ferreira, L.F.R., 2017. Ocorrência de diclofenaco e naproxeno em água superficial no município de Três Lagoas (MS) e a influência da temperatura da água na detecção desses anti-inflamatórios. Eng. Sanit. Ambient. 22, 429-435.

Cheng, N., Wang, B., Wu, P., Lee, X., Xing, Y., Chen, M., Gao, B., 2021. Adsorption of emerging contaminants from water and wastewater by modified biochar: A review. Environ. Pollut. 273, 116448. https://doi.org/10.1016/j.envpol.2021.116448.

Feng, X., Qiu, B., Dang, Y., Sun, D., 2021. Enhanced adsorption of naproxen from aquatic environments by β-cyclodextrin-immobilized reduced graphene oxide. Chem. Eng. J. 412, 128710. https://doi.org/10.1016/j.cej.2021.128710.

Freundlich, H., 1906. Over the adsorption in solution. J. Phys. Chem-us. 57, 385-470.

Garg, V.K., Kumar, R., Gupta, R., 2004. Removal of .malachite green dye from aqueous solution by adsorption using agro-industry waste: A case study of Prosopis cineraria.

555 Dyes Pigments. 62, 1-10. https://doi:10.1016/S0143-7208(03)00224-9.

556 Hiew, B.Y.Z., Lee, L.Y., Lee, X.J., Gan, S., Thangalazhy-Gopakumar, S., Lim, S.S., Pan,
557 G.T., Yang, T.C.K., 2019. Adsorptive removal of diclofenac by graphene oxide:
558 Optimization, equilibrium, kinetic and thermodynamic studies. J. Taiwan. Inst. Chem. E.
559 98, 150–162. https://doi.org/10.1016/j.jtice.2018.07.034.

560 Ho, Y.S., Mckay, G., 1999. Pseudo-second order model for sorption processes. Process.
561 Biochem. 34, 451-465. https://doi.org/10.1016/S0032-9592(98)00112-5.

562 Hong, J., Zhu, Z., Lu, H., Qiu, Y., 2014. Synthesis and arsenic adsorption performances
563 of ferric-based layered double hydroxide with α-alanine intercalation. Chem. Eng. J. 252,
564 267-274. https://doi.org/10.1016/j.cej.2014.05.019.

565 Huang, X.Y., Bin, J.P., Bu, H.T., Jiang, G.B., Zeng, M.H., 2011. Removal of anionic dye
566 eosin y from aqueous solution using ethylenediamine modified chitosan. Carbohyd.
567 Polym. 84, 1350-1356. https://doi.org/10.1016/j.carbpol.2011.01.033.

568 Isique, W.D., Silva, T.S.; Matsumoto, T., 2017. A composite of polyethylene
569 terephthalate and sugarcane ash-coated $FeSO_4$. 7H2O (PETSCA/Fe) as a low-cost
570 adsorbent material. Mater. Lett. 188, 423–425.
571 http://dx.doi.org/10.1016/j.matlet.2016.11.068.

572 Kamranifar, M., Naghizadeh, A., 2017. Montmorillonite nanoparticles in removal of
573 textile dyes from aqueous solutions: study of kinetics and thermodynamics. Iran. J. Chem.
574 Chem. Eng. 36, 127-137. https://doi.org/10.30492/IJCCE.2017.27402.

575 Kurtulbaş, E., Bilgin, M., Şahin, S., Bayazit, Ş.S., 2017. Comparison of different
576 polymeric resins for naproxen removal from wastewater. J. Mol. Liq. 241, 633-637.
577 https://doi.org/10.1016/j.molliq.2017.06.070.

578 Langmuir, I., 1917. The constitution and fundamental properties of solids and liquids.
579 Part II.-Liquids. J. Frankl. Inst. 184, 721. https://doi.org/10.1021/ja02254a006.

Lin, X., Xu, J., Keller, A.A., He, L., Gu, Y., Zheng, W., Sun, D., Lu, Z., Huang, J., Huang, X., Li, G., 2020. Occurrence and risk assessment of emerging contaminants in a water reclamation and ecological reuse project. Sci. Total Environ. 744, 140977. https://doi.org/10.1016/j.scitotenv.2020.140977.

Mian, H.R., HU, G., Hewage, K., Rodriguez, M.J., Sadiq, R., 2021. Drinking water quality assessment in distribution networks: A water footprint approach. Sci. Total Environ. 775, 145844. https://doi.org/10.1016/j.scitotenv.2021.145844.

Moreira, S.A., 2008. Adsorção de íons metálicos de efluente aquoso usando bagaço do pedúnculo de caju: estudo de batelada e coluna de leito fixo. [s.l.] Universidade Federal do Ceará.

Moreira, B.J., Yokoya, J.M.C., Gaitani, C.M., 2014. Microextração Líquido-Líquido Dispersiva (DLLME): fundamentos e aplicações. Sci. Chromatographica. 6, 186-204. https://doi/10.4322/sc.2015.005.

Nascimento, R.F., Lima, A.C.A., Vidal, C.B., Melo, D.Q., Raulino, G.S.C., 2020. Adsorção: Aspectos teóricos e aplicações ambientais. 2° edição. Fortaleza: Imprensa Universitária da Universidade Federal do Ceará (UFC). 309p.

Pap, S., Taggart, M.A., Shearer, L., Li, Y., Radovic, S., Sekulica, M.T., 2021. Removal behaviour of NSAIDs from wastewater using a P-functionalised microporous carbon. Chemosphere. 264, 128439. https://doi.org/10.1016/j.chemosphere.2020.128439.

Nodeh, M.K.M., Kanani, N., Abadi, E.B., Sereshti, H., Barghi, A., Rezania, S., Bidhendi, G.N., 2021. Equilibrium and kinetics studies of naproxen adsorption onto novel magnetic graphene oxide functionalized with hybrid glycidoxy-amino propyl silane. Environ. Challenges. 4, 100106. https://doi.org/10.1016/j.envc.2021.100106.

Phasuphan, W., Praphairaksit, N., Imyim, A., 2019. Removal of ibuprofen, diclofenac, and naproxen from water using chitosan-modified waste tire crumb rubber. J. Mol. Liq.

294, 111554. https://doi.org/10.1016/j.molliq.2019.111554.

Rafati, L., Ehrampoush, M.H., Rafati, A.A., Mokhtari, M., Mahvi, A.H., 2016. Modeling of adsorption kinetic and equilibrium isotherms of naproxen onto functionalized nano-clay composite adsorbent. J. Mol. Liq. 224, 832-841. https://doi.org/10.1016/j.molliq.2016.10.059.

Rasheed, T., Ahmad, N., Nawaz, S., Sher, F., 2020. Photocatalytic and adsorptive remediation of hazardous environmental pollutants by hybrid nanocomposites. Case Stud. Chem. Environ. Engineering. 2, 100037. https://doi.org/10.1016/j.cscee.2020.100037.

Rathi, B.S., Kumar, P.S., Show, P.L., 2021. A review on effective removal of emerging contaminants from aquatic systems: Current trends and scope for further research. J. Hazard. Mater. 409, 124413. https://doi.org/10.1016/j.jhazmat.2020.124413.

Ravi, S., Choi, Y., Choe, J.K., 2020. Novel phenyl-phosphate-based porous organic polymers for removal of pharmaceutical contaminants in water. Chem. Eng. J. 379, 122290. https://doi.org/10.1016/j.cej.2019.122290.

Salomão, G.R., Américo-Pinheiro, J.H.P., Isique, D., Torres, N.H., Cruz, I.A., Ferreira, L.F.R., 2021. Diclofenac removal in water supply by adsorption on composite low-cost material. Environ. Technol. 42, 2095-2111. https://doi.org/10.1080/09593330.2019.1692078.

Song, J.Y., Bhadra, B.N., Jhung, S.H., 2017. Contribution of H-bond in adsorptive removal of pharmaceutical and personal care products from water using oxidized activated carbon. Micropor. Mesopor. Mat. 243, 221-228. https://10.1016/j.micromeso.2017.02.024.

Smiljanic, D., Gennaro, B., Daković, A., Galzerano, B., Germinario, C., Izzo, F., Rottinghaus, G.E., Langella, A., 2021. Removal of non-steroidal anti-inflammatory drugs from water by zeolite-rich composites: The interference of inorganic anions on the

630 ibuprofen and naproxen adsorption. J. Environ. Manage. 286, 112168. https://doi:
631 10.1016/j.jenvman.2021.112168.
632 Souza, R.M., Quesada, H.B., Cusioli, L.F., Fagundes-klen, M.R., Bergamasco, R., 2021.
633 Adsorption of non-steroidal anti-inflammatory drug (NSAID) by agro-industrial by-
634 product with chemical and thermal modification: Adsorption studies and mechanism. Ind.
635 Crop. Prod. 161, 113200. https://doi.org/10.1016/j.indcrop.2020.113200.
636 Tomul, F., Arslan, Y., Kabak, B., Trak, D., Kendüzler, E., Lima, E.C., Tran, H.N., 2020.
637 Peanut shells-derived biochars prepared from different carbonization processes:
638 Comparison of characterization and mechanism of naproxen adsorption in water. Sci.
639 Total Environ. 726, 137828. https://doi.org/10.1016/j.scitotenv.2020.137828.
640 Vieira, T., Becegato, V.A., Paulino, A.T., 2021. Equilibrium Isotherms, Kinetics, and
641 Thermodynamics of the Adsorption of 2,4-Dichlorophenoxyacetic Acid to Chitosan-
642 Based Hydrogels. Water. Air. Soil. Poll. 232, 1-16. https://doi.org/10.1007/s11270-021-
643 05021-6.
644 Xiong, P., Zhang, H., Li, G., Liao, C., Jiang, G., 2021. Adsorption removal of ibuprofen
645 and naproxen from aqueous solution with Cu-doped Mil-101(Fe). Sci. Total Environ.
646 797, 149179. https://doi.org/10.1016/j.scitotenv.2021.149179.